Mathematical
Institute

Controlling the variance of the Jacobian's spectrum

Theories of Deep Learning: C6.5,
Lecture / Video 6

Prof. Jared Tanner
Mathematical Institute
University of Oxford

Oxford
Mathematics

Random DNNs hidden layer outputs

Norm of hidden layer outputs

The DNN with weight matrices $W^{(\ell)}$ and bias vectors $b^{(\ell)}$ with Gaussian entries $\mathcal{N}(0, \sigma_w^2)$ and $\mathcal{N}(0, \sigma_b^2)$

$$h^{(\ell)} = W^{(\ell)} z^{(\ell)} + b^{(\ell)}, \qquad z^{(\ell+1)} = \phi(h^{(\ell)}), \qquad \ell = 0, \ldots, L-1,$$

has computable map $R(\rho)$ of how the correlation between two inputs evolve through the layers. The stability of a point and its perturbation is determined by
$\chi := \frac{\partial R(\rho)}{\partial \rho}|_{\rho=1} = \sigma_w^2 \int Dz[\phi'(\sqrt{q^*}z)^2]$.

- χ $le1$: locally stable and points which are sufficiently correlated all converge, with depth, to the same point.
- $\chi > 1$: small perturbations are unstable with nearby points become uncorrelated with depth.

`https://arxiv.org/pdf/1606.05340.pdf`

Stability of pre-activation lengths (Pennington et al. 18')

The "Edge of Chaos Curve" for $\phi(\cdot) = tanh(\cdot)$.

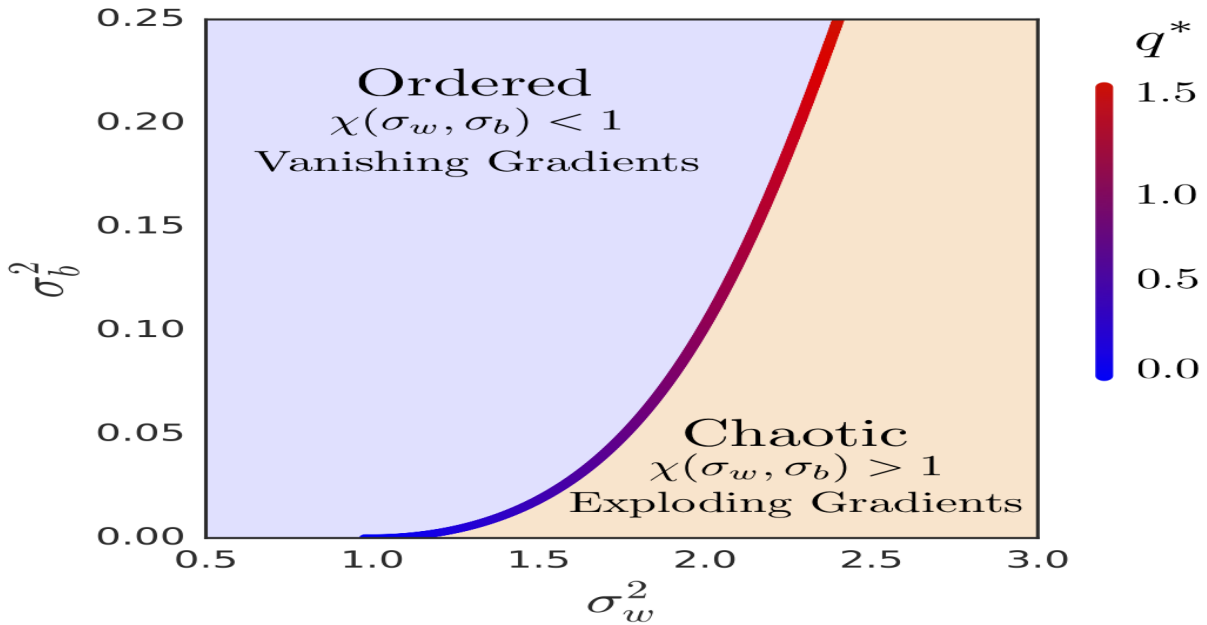

Figure 1: Order-chaos transition when $\phi(h) = \tanh(h)$. The critical line $\chi = 1$ determines the boundary between the two phases. In the chaotic regime $\chi > 1$ and gradients explode while in the ordered regime $\chi < 1$ and we expect gradients to vanish. The value of q^* along this line is shown as a heatmap.

https://arxiv.org/pdf/1802.09979.pdf

The Jacobian of the feed forward net is given by

$$J = \frac{\partial z^{(L)}}{\partial x^{(0)}} = \Pi_{\ell=0}^{L-1} D^{(\ell)} W^{(\ell)}$$

where $D^{(\ell)}$ is diagonal with entries $D_{ii}^{(\ell)} = \phi'(h_i^{(\ell)})$.
Moreover, for the sum of squares loss, the gradient is computed as

$$\delta_\ell = D^\ell (W^{(\ell)})^T \delta_{\ell+1} \quad \text{and} \quad \delta_L = D^{(L)} \text{grad}_{h^{(L)}} \mathcal{L}.$$

which gives the formula for computing the δ_ℓ for each layer as

$$\delta_\ell = \left(\Pi_{k=\ell}^{L-1} D^{(k)} (W^{(k)})^T \right) D^{(L)} \text{grad}_{h^{(L)}} \mathcal{L}.$$

and the resulting gradient $\text{grad}_\theta \mathcal{L}$ with entries as

$$\frac{\partial \mathcal{L}}{\partial W^{(\ell)}} = \delta_{\ell+1} \cdot h_\ell^T \quad \text{and} \quad \frac{\partial \mathcal{L}}{\partial b^{(\ell)}} = \delta_{\ell+1}$$

UNIVERSITY OF OXFORD
Mathematical Institute

In the infinite width limit, the average trace of $(DW)^T(DW)$ is the average of the singular values

$$\chi = N^{-1}\left\langle \mathrm{Tr}((\mathrm{DW})^\top \mathrm{DW})\right\rangle$$

The growth of a perturbation is given by the expected mean singular value of $J^T J$ from one layer to the next which is given by

$$\chi = \sigma_w^2 \int (2\pi)^{-1/2} \phi'\left(\sqrt{q^{(\star)}} z\right)^2 e^{-z^2/2} dz.$$

Consider the spectrum of $J^T J$ more fully, in particular how it varies around its expected value.

`https://arxiv.org/pdf/1606.05340.pdf`

Spectrum of the Jacobian pt. 1(Pennington et al. 18')

How to compute the product of $D^{(\ell)}W^{(\ell)}$

Mathematical Institute

Computing the spectrum of products of matrices, e.g. for $J = \frac{\partial z^{(L)}}{\partial x^{(0)}} = \Pi_{\ell=0}^{L-1} D^{(\ell)} W^{(\ell)}$ where $D_{ii}^{(\ell)} = \phi'(h_i^{(\ell)})$.

Stieltjes and $\mathcal{S}$ Transforms

For $z \in \mathbb{C}/\mathbb{R}$ the Stieltjes Transform, $G_\rho(z)$, of a probability distribution and its inverse are given by

$$G_\rho(z) = \int_{\mathbb{R}} \frac{\rho(t)}{z-t} dt \quad \text{and} \quad \rho(\lambda) = -\pi^{-1} \lim_{\epsilon \to 0_+} Imag(G_\rho(\lambda + i\epsilon)).$$

The Stieltjes Transform and moment generating function are related by $M_\rho(z) := zG_\rho(z) - 1 = \sum_{k=1}^{\infty} \frac{m_k}{z^k}$, and the $\mathcal{S}$ Transform is defined as $S_\rho(z) = \frac{1+z}{zM_\rho^{-1}(z)}$. The $\mathcal{S}$ Transform has the property that if ρ_1 and ρ_2 are freely independent then $\mathcal{S}_{\rho_1\rho_2} = \mathcal{S}_{\rho_1}\mathcal{S}_{\rho_2}$.

`https://arxiv.org/pdf/1802.09979.pdf`

The $\mathcal{S}$ Transform of JJ^T with $J = \frac{\partial z^{(L)}}{\partial x^{(0)}} = \Pi_{\ell=0}^{L-1} D^{(\ell)} W^{(\ell)}$ is then given by

$$\mathcal{S}_{JJ^T} = \mathcal{S}_{D^2}^L \mathcal{S}_{W^T W}^L.$$

This can be computed through the moments $M_{JJ^T}(z) = \sum_{k=1}^{\infty} \frac{m_k}{z^k}$, $M_{D^2}(z) = \sum_{k=1}^{\infty} \frac{\mu_k}{z^k}$, where

$$\mu_k = \int (2\pi)^{-1/2} \phi' \left(\sqrt{q^{(\star)}} z \right)^{2k} e^{-z^2/2} dz.$$

In particular: $m_1 = (\sigma_w^2 \mu_1)^L$ and
$m_2 = (\sigma_w^2 \mu_1)^{2L} L(\mu_2^{-1} \mu_1^2 + L^{-1} - 1 - s_1)$.
Importantly, $\sigma_w^2 \mu_1 = \chi$ is the growth factor we observed with the edge of chaos, requiring $\chi = 1$ to avoid rapid convergence of correlations to fixed points.
`https://arxiv.org/pdf/1802.09979.pdf`

Nonlinear activation stability (Pennington et al. 18')

Examples of moment generating functions

Table 1: Properties of Nonlinearities

	$\phi(h)$	$M_{D^2}(z)$	μ_k	σ_w^2	$\sigma^2_{JJ^T}$
Linear	h	$\frac{1}{z-1}$	1	1	$L\,(-s_1)$
ReLU	$[h]_+$	$\frac{1}{2}\frac{1}{z-1}$	$\frac{1}{2}$	2	$L\,(1-s_1)$
Hard Tanh	$[h+1]_+ - [h-1]_+ - 1$	$\mathrm{erf}(\frac{1}{\sqrt{2q^*}})\frac{1}{z-1}$	$\mathrm{erf}(\frac{1}{\sqrt{2q^*}})$	$\frac{1}{\mathrm{erf}(\frac{1}{\sqrt{2q^*}})}$	$L\,(\frac{1}{\mathrm{erf}(\frac{1}{\sqrt{2q^*}})} - 1 - s_1)$
Erf	$\mathrm{erf}(\frac{\sqrt{\pi}}{2}h)$	$\frac{1}{\sqrt{\pi q^* z}}\Phi\left(\frac{1}{z}, \frac{1}{2}, \frac{1+\pi q_*}{\pi q_*}\right)$	$\frac{1}{\sqrt{1+\pi k q_*}}$	$\sqrt{1+\pi q^*}$	$L\,(\frac{1+\pi q^*}{\sqrt{1+2\pi q^*}} - 1 - s_1)$

Where $M_{D^2}(z) = \sum_{k=1}^{\infty} \frac{\mu_k}{z^k}$ with $\mu_k = \int (2\pi)^{-1/2} \phi'\left(\sqrt{q^{(\star)}} z\right)^{2k} e^{-z^2/2} dz$.

Recall that $m_1 = \chi^L$ is the expected value of the spectrum of JJ^T; while the variance of the spectrum of JJ^T is given by $\sigma^2_{JJ^T} = m_2 - m_1^2 = L(\mu_2 \mu_1^{-2} - 1 - s_1)$, where for W Gaussian $s_1 = -1$ and for W orthogonal $s_1 = 0$.

Linear $\phi(\cdot)$: $q^* = \sigma_w^2 q^* + \sigma_b^2$, has fixed point $(\sigma_w, \sigma_b) = (1, 0)$.

ReLU $\phi(\cdot)$: $q^* = \frac{1}{2}\sigma_w^2 q^* + \sigma_b^2$, has fixed point $(\sigma_w, \sigma_b) = (\sqrt{2}, 0)$.

Hard Tanh and Erf have curves as fixed points $\chi(\sigma_w, \sigma_b)$.

`https://arxiv.org/pdf/1802.09979.pdf`

Distribution of activations $\phi'(z)$ (Pennington et al. 18')

$$\mu_k = \int (2\pi)^{-1/2} \phi' \left(\sqrt{q^{(\star)}} z \right)^{2k} e^{-z^2/2} dz.$$

University of Oxford
Mathematical Institute

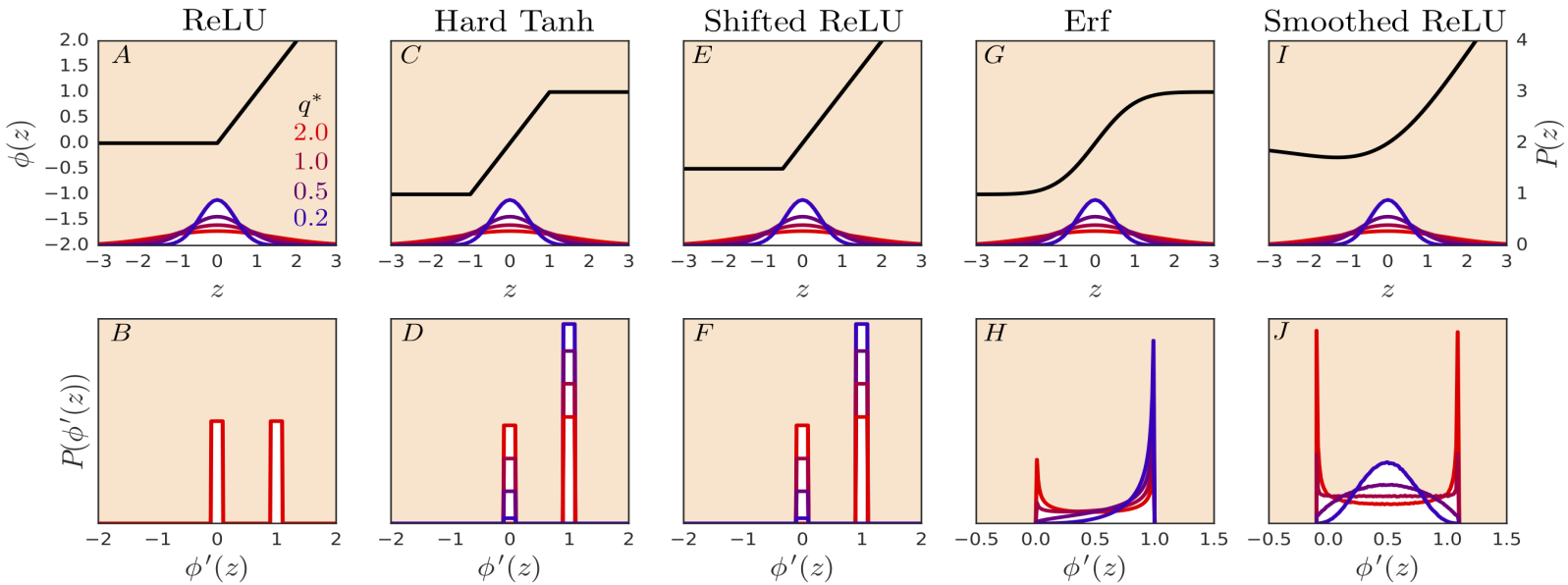

Figure 3: Distribution of $\phi'(h)$ for different nonlinearities. The top row shows the nonlinearity, $\phi(h)$, along with the Gaussian distribution of pre-activations h for four different choices of the variance, q^*. The bottom row gives the induced distribution of $\phi'(h)$. We see that for ReLU the distribution is independent of q^*. This implies that there is no stable limiting distribution for the spectrum of $\mathbf{J}\mathbf{J}^T$. By contrast for the other nonlinearities the distribution is a relatively strong function of q^*.

https://arxiv.org/pdf/1802.09979.pdf

Definition (scaled-bounded activations)

We refer to the set of activation functions $\phi : \mathbb{R} \to \mathbb{R}$ which satisfy the following properties as scaled-bounded activations.

1. Continuous.
2. Odd, meaning that $\phi(z) = -\phi(-z)$ for all $z \in \mathbb{R}$.
3. Linear around the origin and bounded: in particular there exists $a, k \in \mathbb{R}_{>0}$ such that $\phi(z) = kz$ for all $z \in [-a, a]$ and $\phi(z) \leq ak$ for all $z \in \mathbb{R}$.
4. Twice differentiable at all points $z \in \mathbb{R} \backslash \mathcal{D}$, where $\mathcal{D} \subset \mathbb{R}$ is a finite set. Furthermore $|\phi'(z)| \leq k$ for all $z \in \mathbb{R} \backslash \mathcal{D}$.

`https://arxiv.org/abs/2105.07741`

Correlation map and variance convergence (Murray et al. 21')

Increasing the linear region drives the Jacobian spectra to 1

UNIVERSITY OF OXFORD
Mathematical Institute

Theorem (Murray 21')

Let ϕ be a scaled-bounded activation, $\sigma_b^2 > 0$, $\chi_1 := \sigma_w^2 \mathbb{E}[\phi'(\sqrt{q^*}Z)^2] = 1$ where $q^* > 0$ is a fixed point of V_ϕ. Let inputs x satisfy $||\mathrm{x}||_2^2 = q^*$.
Then as $y := \sigma_b^2/a^2 \to 0$, both

$$\max_{\rho\in[0,1]} |R_{\phi,q^*}(\rho) - \rho|, \left|\mu_2/\mu_1^2 - 1\right| \to 0,$$

with rates available in Murray 21'.

Note that this is independent of details of $\phi(\cdot)$ outside its linear region $[-a, a]$. Best performance is observed with $a \sim 3$, or preferably a decreasing from about 5 to 2 during training.
`https://arxiv.org/abs/2105.07741`

Training very DNNs with Shtanh (Murray et al. 21')

Improved accuracy with dynamic linearity decay

UNIVERSITY OF OXFORD
Mathematical Institute

Test accuracy of a trained very deep feed forward net on CIFAR-10.

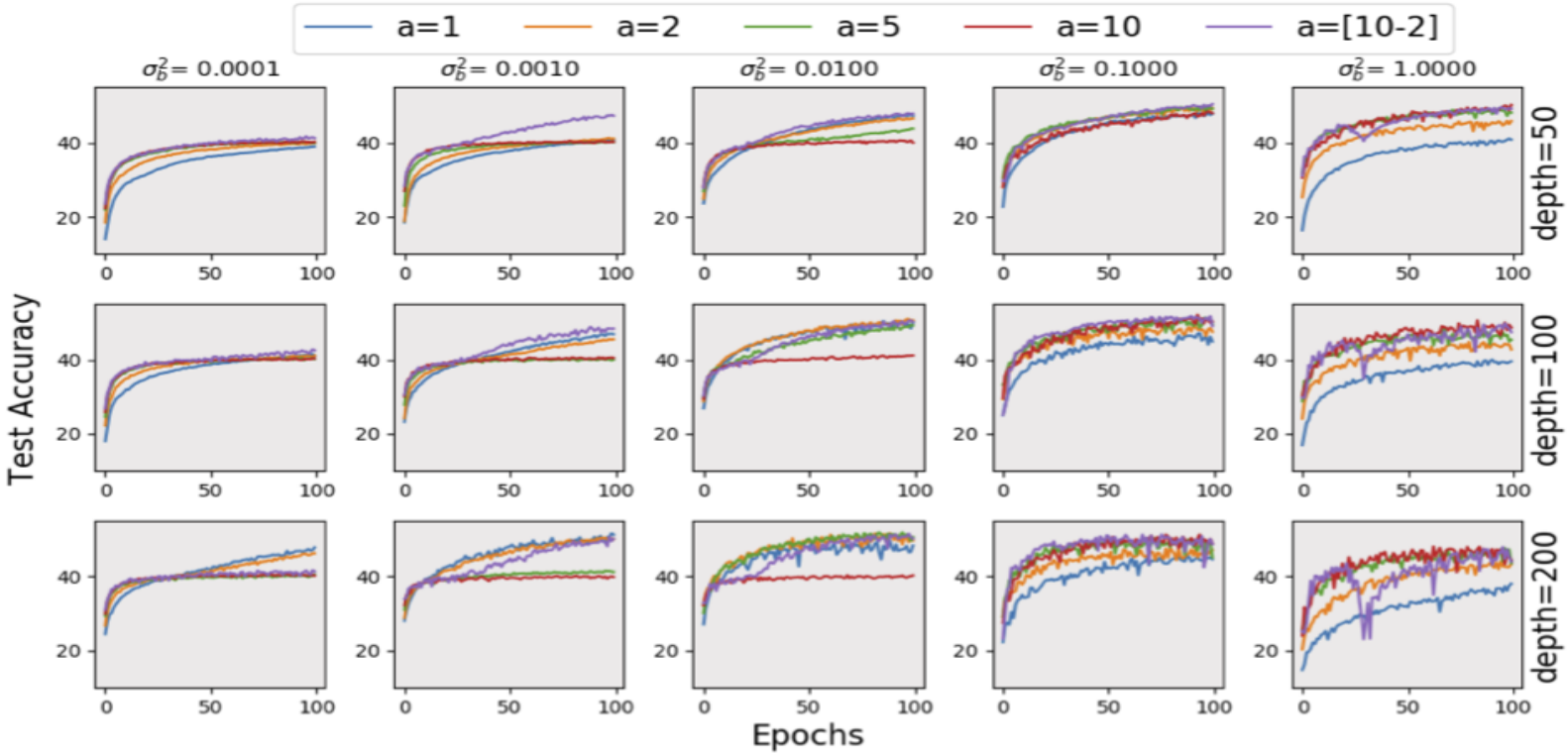

(b) Shtanh with orthogonal initialisation

https://arxiv.org/abs/2105.07741

Distribution of Jacobian spectra (Pennington et al. 18')

Observed universality of spectra based on $\phi(\cdot)$

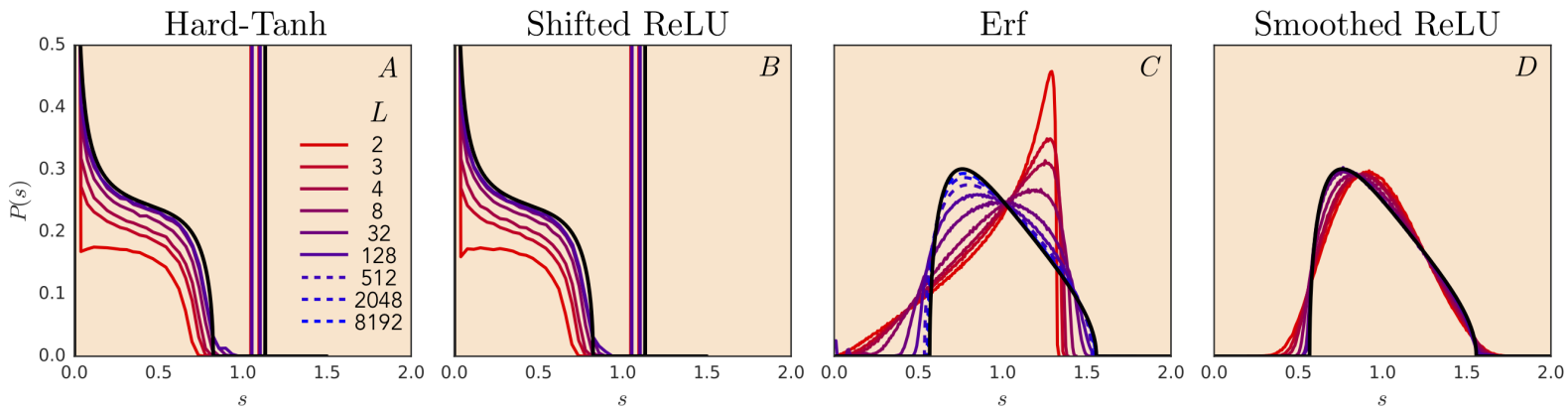

Figure 4: Two limiting universality classes of Jacobian spectra. Hard Tanh and Shifted ReLU fall into one class, characterized by Bernoulli-distributed $\phi'(h)^2$, while Erf and Smoothed ReLU fall into a second class, characterized by a smooth distribution for $\phi'(h)^2$. The black curves are theoretical predictions for the limiting distributions with variance $\sigma_0^2 = 1/4$. The colored lines are emprical spectra of finite-depth width-1000 orthogonal neural networks. The empirical spectra converge to the limiting distributions in all cases. The rate of convergence is similar for Hard-Tanh and Shifted ReLU, whereas it is significantly different for Erf and Smoothed Relu, which converge to the same limiting distribution along distinct trajectories. In all cases, the solid colored lines go from shallow $L = 2$ networks (red) to deep networks (purple). In all cases but Erf the deepest networks have $L = 128$. For Erf, the dashed lines show solutions to (15) for very large depth up to $L = 8192$.

`https://arxiv.org/pdf/1802.09979.pdf`

Summary of random DNN initialisation

Dependence between $\sigma_w, \sigma_b, \phi(\cdot)$

UNIVERSITY OF OXFORD
Mathematical Institute

- Poole et al. 16' showed pre-activation output is well modelled as Gaussian with variance q^* determined by $\sigma_w, \sigma_b, \phi(\cdot)$. Moreover, the correlation between two inputs follows a similar map with correlations converging to a fixed point, with the behaviour determined in part by χ where $\chi = 1$ avoids correlation to the same point, or nearby points diverging. `https://arxiv.org/pdf/1606.05340.pdf`
- Pennington et al 18' showed more generally how to compute the moments for the Jacobian spectra, where $\chi = 1$ is needed to avoid exponential growth or shrinkage with depth of gradients. `https://arxiv.org/pdf/1802.09979.pdf`

Further associated reading 1 of 2

Related results

- Identifying natural depth scales of information propagation
  `https://arxiv.org/pdf/1611.01232.pdf`
- Further details on the role of activation functions
  `https://arxiv.org/pdf/1902.06853.pdf`
- Principles for selecting activation functions
  `https://arxiv.org/pdf/2105.07741.pdf`

Further associated reading 2 of 2

Convergence of representations at each layer of a neural network to a Gaussian Process & wider reading

- Early results on correlation of inputs (Chapter 2 in particular) `https://www.cs.toronto.edu/~radford/ftp/thesis.pdf`
- Rigorous treatment of Gaussian Process perspective, infinite width `https://arxiv.org/pdf/1711.00165.pdf`
- Rigorous treatment of Gaussian Process perspective, finite width `https://arxiv.org/pdf/1804.11271.pdf`
- Higher order terms and width proportional to depth scaling `https://arxiv.org/pdf/2106.10165.pdf`
- Specifics for random ReLU nets `https://arxiv.org/pdf/1801.03744.pdf` `https://arxiv.org/pdf/1803.01719.pdf`